CIÊNCIA e NATURA
ISSN 2179-460X
OPEN ACCESS
Ci. e Nat., Santa Maria, v. 48, e87939, 2022 • https://doi.org/10.5902/2179460X87939
Submitted: 14/06/2024 • Approved: 14/08/2024 • Published: 26/08/2026

Geosciences

Characterizing the 2019-2021 drought in southern and southeastern Brazil using S-TRACK method

Caracterização da seca 2019-2021 no sul e sudeste do Brasil utilizando o método S-TRACK

Osmar Toledo Bonfim [I], **Vanessa Ferreira** [I], **Rafael Maroneze** [I], **Roilan Valdes** [II], **Luca Mortarini** [III]

[I] Universidade Federal do Pampa, Bagé, RS, Brasil
[II] ENGIE Brasil Energia, Florianópolis, SC, Brasil
[III] Institute of Atmospheric Sciences and Climate, National Research Council (ISAC-CNR), Bologna, BO, Itália

ABSTRACT

The period from 2019 to 2021 witnessed an enduring and severe drought that impacted southeast South America. Initially characterized as a meteorological drought, its influence later extended across the entire hydrological cycle. This paper explores the application of the S-TRACK method to monitor and characterize the 2019/21 drought in Southern Brazil (SB) and Southeast Brazil (SEB). Monthly precipitation data from reanalyses and satellites, alongside the Standardized Precipitation Index (SPI) for drought quantification, are utilized. Precipitation datasets, validated against rain gauge records, highlight ERA-5 and CHIRPS as having the highest correlation in SB, and CHIRPS and PERSIANN exhibiting the best agreement in SEB. The utilization of the S-TRACK method for spatial drought tracking revealed the temporal dynamics of the drought events, with three significant episodes occurring in 2020/2021. Initially, the onset of the drought was observed in the SB region, characterized by intensities ranging from moderate to extreme. Subsequently, the drought extended northward, reaching its maximum intensity at lower latitudes within the SEB region before either dissipating or experiencing a reduction in both its spatial extent and intensity. The S-TRACK analysis also revealed a pattern of spatial overlap of drought clusters indicating that drought conditions remained stationary for an extended period, especially for the March to May/2020 period.

Keywords: Precipitation deficit; Drought indexes; Spatial tracks; South America

RESUMO

O período de 2019 a 2021 testemunhou uma seca severa e duradoura que impactou o sudeste da América do Sul. Caracterizada inicialmente como uma seca meteorológica, a sua influência estendeu-se posteriormente a todo o ciclo hidrológico. Este artigo explora a aplicação do método S-TRACK para monitorar e caracterizar a seca de 2019/21 no Sul do Brasil (SB) e Sudeste do Brasil (SEB). Foram utilizados dados mensais de precipitação provenientes de reanálises e satélites, juntamente com o Índice Padronizado de Precipitação (SPI) para quantificação da seca. Conjuntos de dados de precipitação, foram validados utilizando dados de estações pluviométricas, destacaram-se o ERA-5 e o CHIRPS como tendo a maior correlação no SB, e o CHIRPS e o PERSIANN apresentando a melhor concordância no SEB. A utilização do método S-TRACK para rastreamento espacial da seca revelou a dinâmica temporal dos eventos de seca, com três episódios significativos ocorrendo em 2020/2021. Inicialmente, observou-se o início da seca na região do SB, caracterizada por intensidades que variam de moderadas a extremas. Posteriormente, a seca estendeu-se para norte, atingindo a sua intensidade máxima em latitudes mais baixas na região SEB antes de se dissipar ou sofrer uma redução tanto na sua extensão espacial como na sua intensidade. A análise S-TRACK também revelou um padrão de sobreposição espacial de aglomerados de secas, indicando que as condições de seca permaneceram estacionárias por um período prolongado, especialmente no período de Março a Maio/2020.

Palavras-chave: Déficit de precipitação; Índices de seca; Rastreamento espacial; América do Sul

1 Introduction

During the period from 2019 to 2021, a prolonged and intense drought affected the southeast South America region. The event initially manifested as a meteorological drought characterized by precipitation deficits, but its persistence also impacted the entire hydrological cycle, profoundly affecting soil moisture, rivers, surface and groundwater reservoirs, as well as regional ecosystems. The effects of this event were widespread, generating significant repercussions in agricultural production, water supply, energy generation, and posing a serious threat to vital ecosystems (DERAL, 2020; Getirana et al., 2021; Naumann et al., 2021). For instance, in the Southern Brazil (SB) and Southeast Brazil (SEB) regions, significant agricultural losses were recorded, with more than 40% of the area being affected. Simultaneously, a notable decline in discharge levels in vital rivers in April 2020, including the Iguaçu, Uruguay, and Paraná rivers, has resulted in limitations affecting both hydropower generation and freshwater supply (Gomes et al., 2021). .

Drought monitoring indices, such as the Standardized Precipitation Index (SPI), play a fundamental role in identifying precipitation scarcity and tracking the development of drought conditions in specific locations. The significance of SPI in drought analysis cannot be underestimated, as it is a valuable tool for quantifying and characterizing the severity of drought conditions and providing information about the spatial extent of these events (Diaz et al., 2020a; Spinoni et al., 2019). However, there is still a lack of consistent methods for continuously tracking drought-affected areas, which, in turn, hinders the assessment of the temporal variations that comprise the spatiotemporal dynamics of this climatic phenomenon.

In this context, the spatial drought tracking method, known as S-TRACK, introduced by Diaz et al. (2018); Herrera-Estrada et al. (2017) and subsequently enhanced by other researchers Diaz et al. (2020a,2); Hosseini et al. (2021); Verhoeven et al. (2022), aims at constructing spatial tracks and trajectories of drought. The S-TRACK method involves three key steps: (1) computation of spatial drought units, also known as areas or clusters; (2) determination of the centroids for these spatial drought units; and (3) establishment of connections between the centroids in the spatiotemporal domain. S-TRACK can help in the understanding on how droughts form, move, and intensify over time, allowing for a more accurate assessment of the risks associated with these extreme climatic events (Diaz et al., 2020a; Herrera-Estrada et al., 2017).

The studies Hosseini et al. (2021); Verhoeven et al. (2022) used the S-TRACK methodology to analyze the spatial characteristics of drought and created trajectories to investigate its spatiotemporal dynamics. These trajectories provided information on the duration, severity, and intensity of drought conditions in Iran and southern Australia, respectively. The results of these studies offer valuable insights that can contribute to the enhancement of preparedness for extreme precipitation events as they become more frequent. Furthermore, they provide authorities and local communities with the opportunity to take proactive measures to mitigate the impacts of droughts.

This study focuses on the identification and characterization of the areas affected by the 2019/21 drought in SB and SEB, highlighting the contribution of the S-TRACK method in investigating this phenomenon and how its application enables a characterization of this drought event.

2 Materials and Methods

2.1 Datasets and study area

The study area includes the states belonging to the Southern (SB) and Southeastern (SEB) regions of Brazil, demarcated by the geographical coordinates 14°15′ to 33°45′ latitude South and 39°40′ to 57°37′ longitude West (figura1). These regions exhibit substantial geographical diversity in climate, vegetation and terrain, and occupy a vast territorial expanse. Cumulatively, they encompass an area of approximately 1.682.676 km², representing approximately 20% of the Brazilian territory.

Figure 1 – Topographic features and location of the Southeast and South regions of Brazil. The states constituting the Southeast region of Brazil are as follows: São Paulo (SP), Rio de Janeiro (RJ), Espírito Santo (ES) e Minas Gerais (MG). And for the Southern Brazil region, the states are: Rio Grande do Sul (RS), Santa Catarina (SC) e Paraná (PR).The abbreviations for each of these states are indicated in the figure

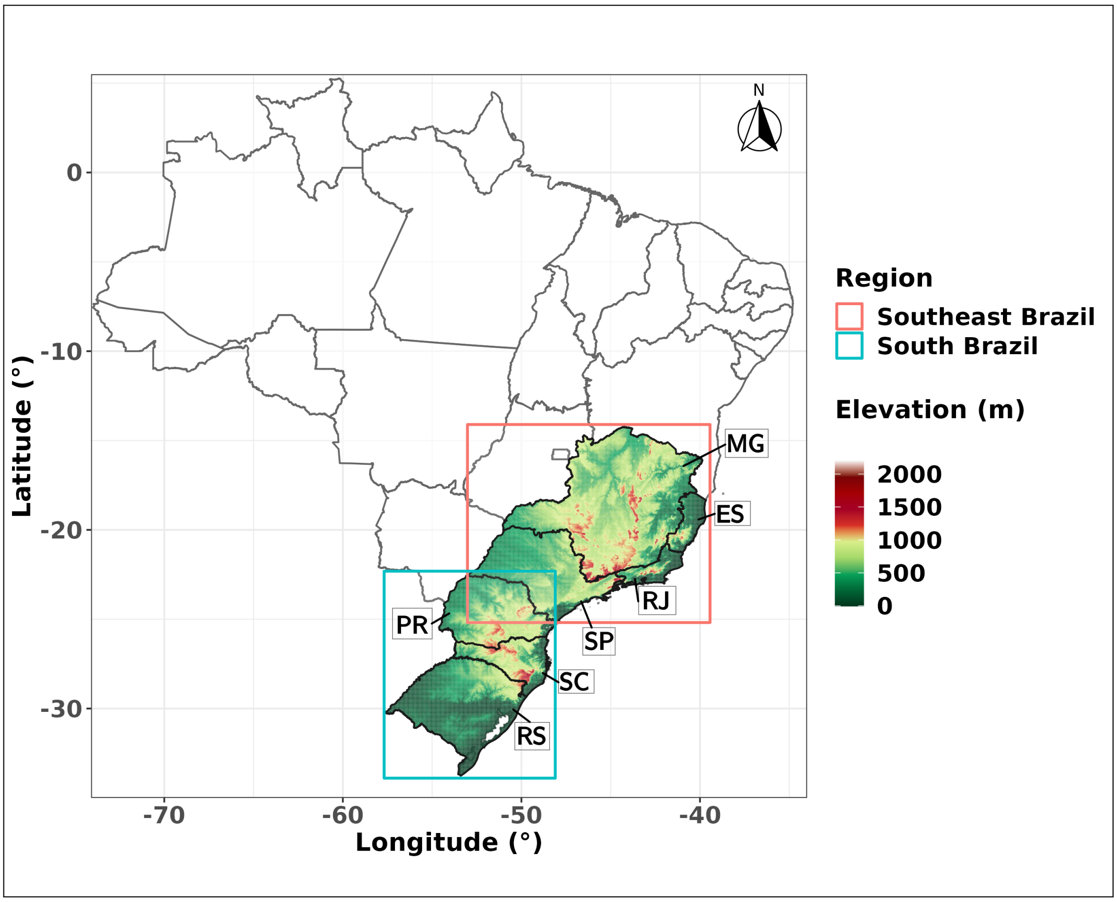

Source: Authors (2024)

To identify areas experiencing dry conditions in the Southern and Southeastern regions of Brazil during the 2019/2021 period, monthly precipitation data were utilized. Given the limited spatial and temporal resolution of meteorological stations in Brazil, precipitation data from reanalyses and satellites were selected due to their higher resolution, providing a significant advantage, especially in terms of area coverage in regions with limited data availability. The selection of datasets was based on two key criteria: good spatial resolution and data availability, resulting in the choice of three distinct datasets.

Two of the datasets were obtained through satellite-based methods. The first one is the Precipitation Estimation from Remotely Sensed Information using Artificial Neural Networks Climate Corrected and Continuous Distributed (PERSIANN-CCS-CDR) system, featuring a spatial resolution of 0.04° and a temporal resolution of half an hour (Sadeghi et al., 2021). The second dataset is the Climate Hazards Group Infrared Precipitation with Stations (CHIRPS), comprising a high-resolution (0.05°) precipitation dataset that integrates multiple sources, including NOAA, CPC, NCDC, and meteorological station data (Funk et al., 2015).

The third dataset consists of precipitation information obtained from ERA-5, the fifth generation of atmospheric reanalysis developed by the European Centre for Medium-Range Weather Forecasts (ECMWF). ERA-5 provides hourly precipitation data with a spatial resolution of 0.25°, along with an extensive and consistent climatic record covering the entire globe (Hersbach et al., 2020).

To validate the precipitation estimates derived from these datasets, historical precipitation data series from the National Institute of Meteorology (INMET) were used. A period of 30 years (1991-2020) was chosen for analysis, as it is considered suitable for climatological statistical analyses.

2.2 Drought characterization

In order to quantify and characterize the extreme drought event, the Standardized Precipitation Index (SPI) was employed at a 3-month scale. Previous studies (Kamruzzaman et al., 2019; Tirivarombo et al., 2018) have highlighted that the SPI is more consistent in representing actual drought conditions when applied at shorter and medium time scales, compared to longer scales (9 and 12-month scale).

The SPI is a simple, flexible, and effective index that allows for the analysis of both wet and dry periods, relying solely on precipitation as the input parameter (Dos Santos et al., 2022; McKee et al., 1993; Rocha et al., 2022).

The SPI is computed based on the accumulated probability of occurrence for each monthly precipitation value. To standardize the data, the Z value is calculated by subtracting the mean precipitation value Pi from the monthly precipitation of the corresponding period ρi, and dividing the result by the standard deviation σi (McKee et al., 1993). As demonstrated by the following equation 1:

$$SPI = \frac{(\rho_i - P_i)}{\sigma_i} \tag{1}$$

The SPI is a standardized indicator that adjusts the precipitation to a statistical distribution over a reference period, enabling the classification of drought and wet conditions using a simple scheme based on standard deviations from the mean. It facilitates the comparison of precipitation magnitude across different locations and time periods, offering an objective measure of precipitation events. Positive SPI values indicate wet condition, while negative values represent dry condition. Table 1 presents the SPI categories, as defined by (McKee et al., 1993).

Table 1 – Classification of dry and wet periods according to the SPI value (McKee et al., 1993).

SPI	**Category**
Extreme wet	$>$2
Severe wet	1,5 to 1,99
Moderate wet	1 to 1,49
Near normal	-0,99 to 0,99
Moderate dry	-1 to -1,49
Severe dry	-1,5 to -1,99
Extreme dry	$<$-2

2.3 Validation of precipitation datasets

The methodology proposed by (Taylor, 2001) and employed by (Yang et al., 2021), offers a concise statistical summary of the agreement between the estimated and observed patterns. The Taylor diagram was employed to evaluate the accuracy of satellite data (CHIRPS, PERSIANN) and reanalysis data (ERA-5) in terms of the spatial distribution of precipitation in the SB and SEB regions. The analysis was based on the temporal series of 3-month SPI (SPI-3) from 1991 to 2020, using observations from INMET meteorological stations as the reference data. This graphical representation considers the correlation coefficient (R), standard deviation amplitude (σ), and Root Mean Square (RMS) difference between the two fields as evaluation metrics. It provides an overview of how well the simulated pattern approximates the observed data.

However, relying solely on the correlation coefficient (R) is insufficient to determine whether two variables share the same range of variation. To assess the quality of the model and quantify the disparity between two variables, the most commonly utilized statistic is the RMS difference E, given by equation 2:

$$RMSE = \left| \frac{1}{N} \sum_{n=1}^{N} (\int_n - \Gamma_n)^2 \right| \quad (2)$$

where: (E) represents the root mean square difference, (N) is the number of data points, ($\int$ n) and (Γ n) are the corresponding values of the two variables being compared.

The root mean square difference provides a measure of the average discrepancy between the observed and predicted values, allowing for a comprehensive evaluation of the model's performance. It takes into account both the magnitude of the differences, providing valuable insights into the accuracy and fit of the model.

The construction of the Taylor diagram entails representing either a half or quarter circle, with the quarter circle being the more commonly used representation. The x and y axes correspond to the measures of (σ), where the (σ) value of the observed data is depicted along the x-axis. The azimuth from the origin to the model is proportionate to the correlation coefficient (R). The distance between the reference point on the diagram and the model point is represented by the value of the root mean square difference (RSME) and standard deviation (σ) of the estimated point is proportional to the radial distance from the reference point.

2.4 Spatial Tracking of Drought

Within the spatial tracking context, drought units are identified through cluster analysis following the application of SPI. To assess whether a cell is experiencing drought, a binary approach is employed, assigning a value of 1 to indicate drought presence and 0 to indicate its absence. This binary representation enables the utilization of pattern recognition techniques that group neighboring cells based on shared characteristics (Corzo Perez et al., 2011). As demonstrated by the following equation 3:

$$DS_t = 1 \text{ if } SPI_t \leq L \quad or \quad 0 \text{ if } SPI_t > L \tag{3}$$

where Ds represents the drought state in each cell at every time step (t), based on the designated threshold value (L).

During this step, the threshold value (L= -1) Spinoni et al. (2019); Tirivarombo et al. (2018) was used to evaluate the occurrence of drought at each grid point. Once the clusters are identified, the largest cluster is chosen, and its corresponding centroid is computed at each time step (t) Diaz et al. (2020a); Hosseini et al. (2021). This characteristic facilitates determining the geographic location of each drought area and tracking its temporal movement by connecting the centroids across consecutive time instances, resulting in the formation of drought tracks that represent the trajectory of the drought.

Two consecutive centroids in time are linked through the application of an algorithm that takes into account the cluster area (A) and the distance between the centroids ($\triangle$ l). Parameter A is defined by the largest cluster with value (L= -1) at the time (t). Parameter $\triangle$ l is defined by the distance between the centroids of the largest cluster at the given time (t) and (t + 1). For the process of connecting the centroids, parameter c was established following the description provided by (Diaz et al., 2020b).

$$\Delta l \leq c = \quad true \ (cluster \ connected) \tag{4}$$

Where parameter (c) represents the 70th percentile of the distance between centroids (Δ l). The union of two centroids is called drought track (Diaz et al., 2020b).

Drought tracking enables the identification of trajectories with defined starting and ending points, providing insights into their main direction. The initial and final locations are determined based on the centroids of the first and last clusters, respectively. The magnitude, or extent, of the drought encountered at each time interval using the S-TRACK method is quantified as a measure, calculated by summing the drought areas over time (t). Additionally, the intensity of the drought is defined by the most frequent category of the SPI at the given time (t).

3 Results

In order to assess the accuracy of precipitation estimates derived from PERSIANN, CHIRPS, and ERA5 in comparison to observed data obtained from INMET meteorological stations, Taylor diagrams were employed to analyze SPI-3 time series in the Southern Brazil (SB) and Southeast Brazil (SEB) regions. The findings, depicted in figure 2, indicate that the estimated data for SB demonstrated more variability, as evidenced by relatively elevated standard deviation values. In terms of correlation (R), the ERA-5 and CHIRPS estimates exhibited the highest magnitudes, approximately 0.90, indicating a very strong correlation. On the other hand, the correlation performance of PERSIANN was found to be moderate, falling below 0.70.

Figure 2 – Taylor diagrams comparing the SPI-3 time series of CHIRPS, PERSIANN, and ERA-5 products with respect to the observed data obtained from INMET meteorological stations for the period of 1991-2020

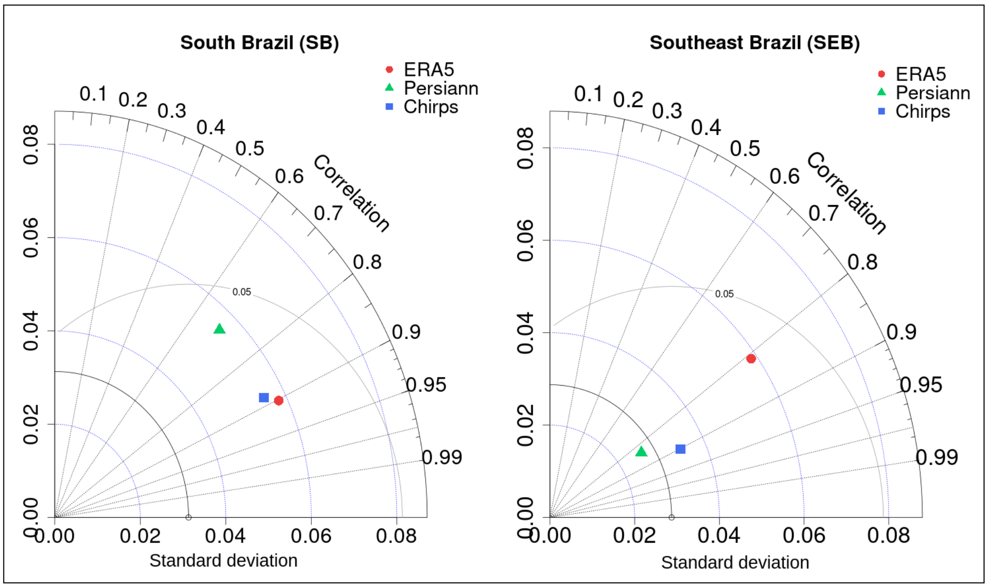

Source: Authors (2024)

The Taylor diagram analysis for SEB demonstrated that the PERSIANN and CHIRPS satellite datasets exhibited the best agreement with the observed data from INMET, as indicated by their similar standard deviations and strong correlations. The correlation coefficient for PERSIANN exceeded 0.80, indicating a strong correlation, while the correlation for CHIRPS was approximately 0.90, denoting a very strong correlation. In contrast, the ERA-5 data showed higher standard deviation values, indicating greater variability in the SEB region. Nevertheless, it still maintained a strong correlation above 0.80. Additionally, the root mean square error (RMSE) values for both regions (SB and SEB) were below 0.05, indicating a good performance of the estimated data in accurately predicting the observed values.

These findings align with the results reported by (Anjum et al., 2022), demonstrating that CHIRPS exhibits greater accuracy in representing the spatial distribution of monthly precipitation compared to PERSIANN. Additionally, other studies including Dos Santos Silva et al., 2023; Jafarpour et al., 2022; Prakash, 2019; Singh et al., 2021 have similarly reported comparable correlation values between the estimated precipitation data and observations obtained from meteorological stations.

Figure 3 illustrates the spatial representation of drought conditions and their severity in the SB and SEB regions. The three spatiotemporal drought distribution maps (Figures 3(A) ERA-5, 3(B) CHIRPS, and 3(C) PERSIANN) exhibited consistent results in identifying the drought event throughout the year 2020. During the December 2019 to February 2020 (DJF) trimester, the SPI-3 maps derived from ERA-5 data revealed an extreme drought occurrence in the southernmost region of SB. However, this extreme drought condition was less pronounced in the CHIRPS and PERSIANN datasets, which categorized it as severe and moderate drought, respectively, covering a smaller proportion of the area.

Figure 3 – Spatial-temporal distribution of meteorological drought in the South and Southeast of Brazil throughout 2019-2020 using SPI-3. (A) ERA-5; (B) CHIRPS; (C) PERSIANN

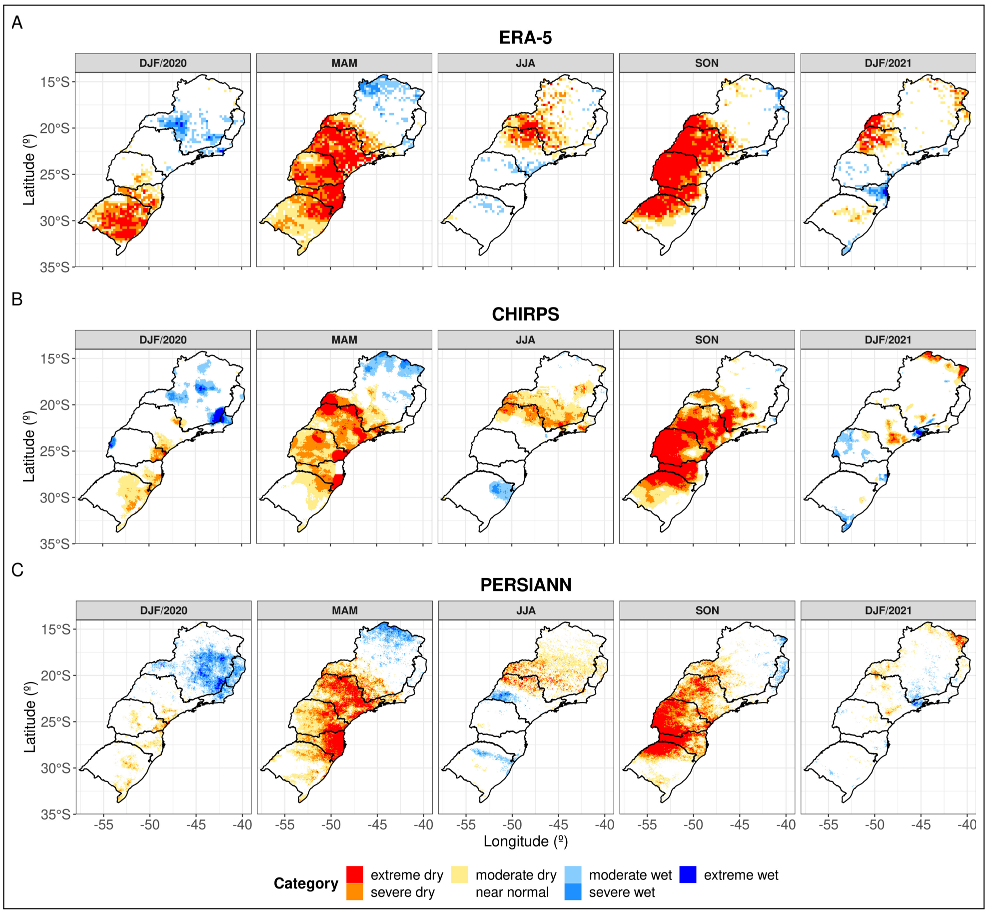

Source: Authors (2024)

During the March to May (MAM) and September to November (SON) trimesters of 2020, the occurrence of extreme drought was primarily concentrated in the central region of the study area, with a greater impact on states located between latitudes

20°S and 30°S. This spatial pattern was consistently observed across the three datasets analyzed. Specifically, in the state of Minas Gerais (MG), the southern region experienced a more severe drought during both trimesters, while the northern part of the state was classified as relatively humid. This behavior can be attributed to the fact that the SEB is located in a transitional zone of the El Niño-Southern Oscillation (ENSO) phenomenon Coelho et al., 2022; Minuzzi et al., 2005.

Figure 4 presents the spatial coverage of drought occurrence throughout the year 2020, quantified by the percentage of the SB and SEB area with SPI-3 values $\leq$ -1, considering the three datasets. The MAM trimester exhibited the most extensive spatial coverage of drought, with approximately 70% of the area affected in the ERA-5 dataset and around 60% in the satellite datasets. In contrast, the May to July (MJJ) trimester had the lowest percentage of area affected by drought, with approximately 15% in all three datasets. Subsequently, there was an increase in the percentage of area affected by drought, reaching around 60% again during the SON trimester, particularly in the CHIRPS dataset.

Figure 4 – Percentage of the area in the South and Southeast regions affected by drought events (SPI-3 $\leq$ -1) throughout 2020

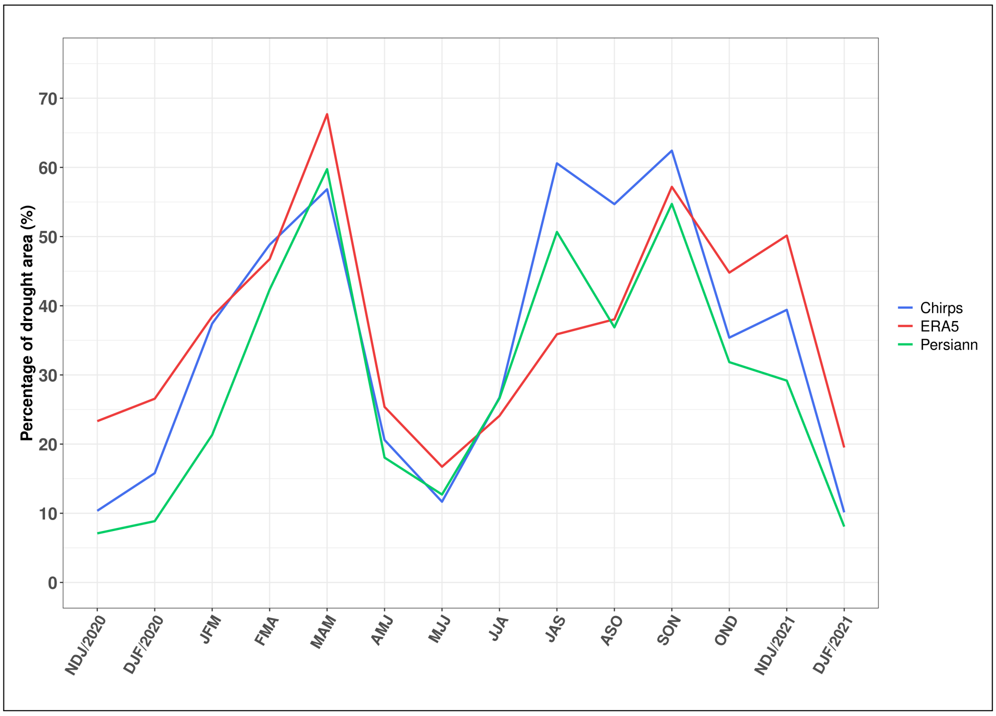

Source: Authors (2024)

The S-TRACK methodology Diaz et al., 2020a,2; Hosseini et al., 2021; Verhoeven et al., 2022 was implemented using the average of the three dataset to evaluate spatiotemporal drought conditions. The results, presented in figure5, demonstrate the spatial tracking of drought in the SB and SEB regions, revealing the occurrence of three main events in 2020/2021, the first two originating in the SB region and the third in the SEB region.

During the November to January (NDJ - 2019/2020) trimester (Figure 5a), the onset of the drought event was observed near latitude 30°S with a moderate intensity. Subsequently, the event advanced northward and reached its peak magnitude and intensity during the MAM trimester near latitude 25°S, being classified as an extreme drought. From DJF 2020/2021 to MAM 2021 (Figure 5a), each of the drought clusters has a spatial overlap with the previous cluster, indicating that the drought clusters remained within the same spatial range. The persistence of centroids in this region suggests that drought conditions remained stationary for an extended period, contributing to the aggravation of drought severity, particularly during the MAM trimester. This is corroborated by the spatial SPI maps figure3, which indicate an expansion and intensification of drought in the SB region between DJF and MAM.

In fact, according to (Getirana et al., 2021), during the MAM period of 2020, the drought in the central-southern region of Brazil led to a deficit of 267 km^3 in water storage compared to the 20-year seasonal average. This water scarcity affected various components of the hydrological system, including rivers, lakes, soil, and aquifers. Furthermore, during this period a significant number of major reservoirs recorded capacities below 20%, leading to significant impacts, particularly in agriculture, energy production, and the provision of potable water to the population.

The drought centroid subsequently shifted further north and settled near latitude 20°S, characterized as a moderate drought. Finally, the drought dissipated during the July to September (JAS) trimester. The drought persisted in a stationary position near 20°S for an extended period, leading to an intensification of its severity during the JJA and JAS trimesters, as depicted in figure3. These observations are consistent with the findings of (Hosseini et al., 2021), who suggested that the persistence of large drought areas in the same region over time could contribute to the severity of droughts during periods characterized by intense drought events.

Figure 5 – Spatial tracking of drought, using the average of the three dataset, calculated based on the distance from the centroid of the largest drought cluster in each quarter of 2020. The size of the circle represents the spatial extent of drought, while the color indicates the intensity. The first event occurred in the NDJ 2019/20 quarter and extended until JAS. The second event began in ASO to OND 2020, and the Third event occurred in the NDJ 2020/21 to DJF 2020/21

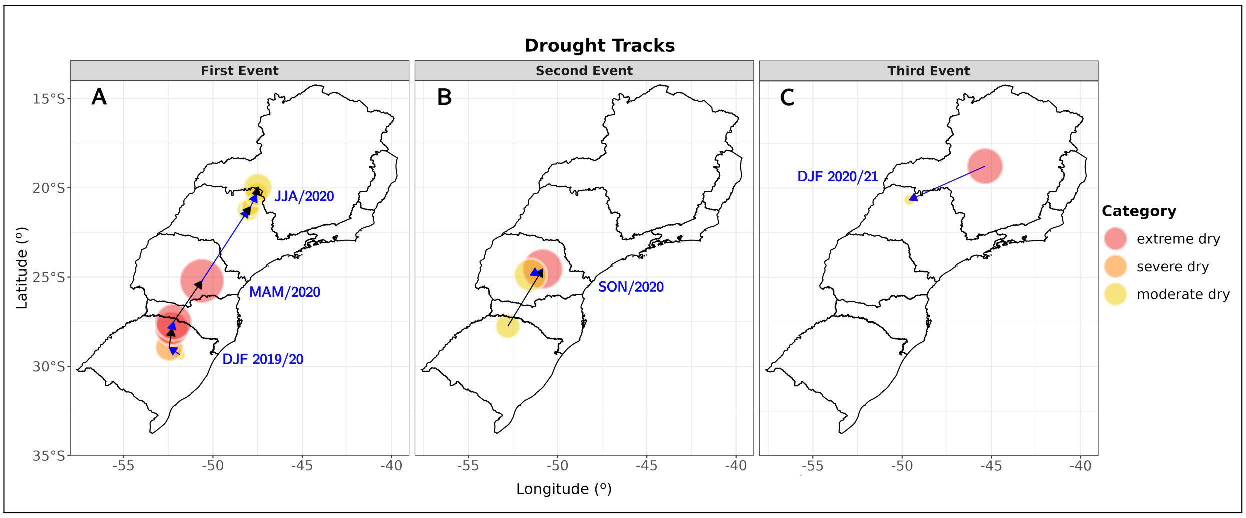

Source: Authors (2024)

During the August to October (ASO) trimester, the second drought event initiated near latitude 27°S with a moderate intensity (Figure 5b). In the following trimesters, the drought episode advanced northward and intensified during the SON trimester near latitude 25°S, resulting in an extreme drought classification. Subsequently, the drought event experienced a slight southwest displacement and diminished in intensity, transitioning back to a moderate drought classification. Again, during SON there is a spatial overlap of the drought clusters, indicating stationary drought conditions. The third event initiated in the November to January (NDJ - 2020/2021) trimester at approximately 19°S latitude (Figure 5c), displaying SPI-3 values within the extreme drought category. However, as the drought event progressed westward, its intensity diminished and dissipated during the subsequent trimester (DJF - 2020/2021). In the first event, the drought propagated over a distance of approximately 1200 km, whereas in the second and third event, its trajectory extended across approximately 500 km.

The S-TRACK analysis also revealed differences in the duration and spatial extent of the drought events. While the second and third events exhibited similar drought severity ratings, they covered smaller areas compared to the first event. The first event covered a large portion of the study area, ranging from 30°S to above 20°S. The second event also remained concentrated within this latitude range, but with a more limited extent. Meanwhile, the third event primarily affected the northern portion of the study area, above 20°S.

Following Diaz et al., 2020a; Herrera-Estrada et al., 2017, the duration of drought events is calculated using the onset and end points of drought paths, along with interconnected drought trails. The first event was characterized by 9 connected centroids, the second by 3, and the third by 2. These numerical values represent the number of months each event persisted and can be used to estimate the duration of the drought episodes. Consequently, the first drought persisted for the longest period, lasting 9 months, which likely contributed to its broader spatial coverage.

4 Conclusion

The analysis of the SPI-3 series for the SB and SEB regions indicated significant drought conditions throughout the year 2020, especially in the Autumn (MAM) and Spring (SON) months, where drought affected approximately 60% to 70% of the study area, classified as severe and extreme in all three datasets used (PERSIANN, CHIRPS, and ERA-5). The S-TRACK method allowed for the construction of a spatial drought trajectory, revealing that this drought comprised three successive events. Initially, the onset of drought was observed at southern latitudes, with intensity ranging from moderate to extreme. As these events progressed northward, their intensity peaked at lower latitudes before dissipating or diminishing in intensity. Using S-TRACK, the duration of each of these drought events was also calculated. The first event persisted for 9 months, the second for 3 and the third persisted for 2 months. The spatial extent of drought events varied, with the first event covering the largest area and the two subsequent events being more localized. One important feature observed is the spatial overlap of the drought clusters, which can be used as an indication of stationary drought conditions over a region. From DJF 2019/2020 to MAM/2020, and during the SON/2020 trimester, the drought clusters remained within the same spatial range, indicating that drought conditions remained stationary for an extended period, contributing to the aggravation of drought severity. In summary, the identification and characterization of drought-prone areas through the SPI-3 and S-TRACK methods can be used as an approach to understand the spatiotemporal dynamics of droughts and help to predict how drought moves over the SB and SEB.

Acknowledgments

This study has been developed as part of the Research and Technological Development Project of the Brazilian electrical energy sector, regulated by National Electric Energy Agency (ANEEL), having received from ENGIE Brasil Energia and Companhia Energética Estreito (P&D-00403-0054/2022).

References

Anjum, M.N., Irfan, M., Waseem, M., Leta, M.K.& Niazi, U.M (2022). Assessment of PERSIANN-CCS, PERSIANN-CDR, SM2RAIN-ASCAT, and CHIRPS-2.0 rainfall products over a semi-arid subtropical climatic region. Water, 14(2), 147. https://doi.org/10.3390/w14020147

Coelho, C., Uvo, C., & Ambrizzi, T.(2002). Exploring the impacts of the tropical Pacific SST on the precipitation patterns over South America during ENSO periods. Theor Appl Climatol, 71, 185–197. https://doi.org/10.1007/s007040200004

Corzo Perez, G.A., Van Huijgevoort, M.H.J., Voß, F., & Van Lanen, H.A.J. (2011) On the spatio-temporal analysis of hydrological droughts from global hydrological models. Hydrology and Earth System Sciences, 15(9), 2963-2978. https://doi.org/10.5194/hess-15-2963-201

DERAL – Departamento de Economia Rural. (2020). Boletim Informativo – Estiagem Histórica no Paraná. https://www.agricultura.pr.gov.br/sites/default/arquivosrestritos /files/documento/2020-05/estiagem18maio2020.pdf. (Accessed May, 2023).

Diaz, V., Corzo Perez, G.A., Van Lanen, H.A.J., & Solomatine, D. (2018). Intelligent drought tracking for its use in machine learning: implementation and first results. In: La Log- gia, G., Freni, G., Puleo, V., De Marchis, M. (Eds.), HIC 2018. 13th International Conference on Hydroinformatics, 3 Palermo: EasyChair. https://doi.org/10. 29007/klgg.

Diaz, V., Perez, G.A.C., Van Lanen, H.A., Solomatine, D., & Varouchakis, E.A. (2020a). An approach to characterize spatio-temporal drought dynamics. Advances in Water Resources, 137, 103512. https://doi.org/10.1016/j.advwatres.2020.103512

Diaz, V., Perez, G.A.C., Van Lanen, H.A., Solomatine, D., & Varouchakis, E.A. (2020b) Characterisation of the dynamics of past droughts. Science of the Total Environment, 718, 134588. https://doi.org/10.1016/j.scitotenv.2019.134588

Dos Santos Silva, F.D., Costa, C.P.W., Franco, V.S., & Gomes, H.B. (2023). Intercomparison of Different Sources of Precipitation Data in the Brazilian Legal Amazon. Climate, 11, 241. https://doi.org/10.3390/cli11120241

Dos Santos, B.C., Sanches, R.G., Moreira, R.M., Bourscheidt, V., & Souza, P.H. (2022). Análise espaço-temporal da precipitação na região central do estado de São Paulo utilizando dados CHIRPS. Revista Brasileira de Geografia Física, 15(05), 2582-2600. https://doi.org/10.26848/rbgf.v15.5.p2582-2600

Funk, C., Peterson, P., Landsfeld, M., Pedreros, D., Verdin, J., & Shukla, S. (2015). The climate hazards infrared precipitation with stations—a new environmental record for monitoring extremes. Sci Data, 2, 150066. https://doi.org/10.1038/sdata.2015.66

Getirana, A., Libonati, R., & Cataldi, M. (2021). Brazil is in water crisis—it needs a drought plan. Nature, 600(7888), 218-220. https://doi.org/10.1038/d41586-021-03625-w

Gomes, M.S., de Albuquerque Cavalcanti, I.F., & Müller, G.V. 2019/2020 drought impacts on South America and atmospheric and oceanic influences. Weather and Climate Extremes, 34, 100404. https://doi.org/10.1016/j.wace.2021.100404.

Herrera-Estrada, J. E., Satoh, Y., & Sheffield, J. (2017). Spatiotemporal dynamics of global drought. Geophysical Research Letters, 44(5), 2254-2263. https://doi.org/10.1002/2016GL071768

Hersbach, H., Bell, B., Berrisford, P., Hirahara, S., Horányi, A., Muñoz-Sabater, J. et al. The ERA5 global reanalysis. (2020). Quarterly Journal of the Royal Meteorological Society, 146(730), 1999-2049. https://doi.org/10.1002/qj.3803

Hosseini, A., Ghavidel, Y., & Farajzadeh, M. (2021). Characterization of drought dynamics in Iran by using S-TRACK method. Theoretical and Applied Climatology, 145(1-2), 661-671. https://doi.org/10.1007/s00704-021-03656-3

Jafarpour, M., Adib, A., & Lotfirad, M. (2022). Improving the accuracy of satellite and reanalysis precipitation data by their ensemble usage. Applied Water Science, 12(9), 232. https://doi.org/10.1007/s13201-022-01750-z

Kamruzzaman, M., Cho, J., Jang, M.W., Hwang, S. Comparative evaluation of standardized precipitation index (SPI) and effective drought index (EDI) for meteorological drought detection over Bangladesh. (2019). Journal of the Korean Society of Agricultural Engineers, 61(1), 145-159. https://doi.org/10.5389/KSAE.2019.61.1.145

McKee, T.B., Doesken, N.J., Kleist, J. (1993). The relationship of drought frequency and duration to time scales. In: Proceedings of the 8th Conference on Applied Climatology. AMS, Boston, MA, 179–184.

Minuzzi, R.B., Sediyama, G.C., Ribeiro, A., & Costa, J. (2005). El Niño: ocorrência e duração dos veranicos do Estado de Minas Gerais. Revista brasileira de engenharia agrícola e ambiental, 9, 364-371. https://doi.org/10.1590/S1415-43662005000300011

Naumann, G., Podesta, G., Marengo, J., Luterbacher, J., Bavera, D., Arias-Muñoz, C., Marinho Ferreira Barbosa, P., Cammalleri, C., Chamorro, L., Cuartas, L.A., De Jager, A., Escobar, C., Hidalgo, C., Leal De Moraes, O.L., Mccormick, N., Maetens, W., Magni, D., Masante, D., Mazzeschi, M., Seluchi, M., De Los Milagros Skansi, M., Spinoni, J., & Toreti, A. The 2019-2021 extreme drought episode in La Plata Basin, EUR 30833 EN, Publications Office of the European Union, Luxembourg. ISBN 978-92-76-47671-9, https://doi:10.2760/346183.

Prakash, S. (2019). Performance assessment of CHIRPS, MSWEP, SM2RAIN-CCI, and TMPA precipitation products across India. Journal of hydrology, 571, 50-59. https://doi.org/10.1016/j.jhydrol.2019.01.036

Rocha, L.H.D.S., Silva, D.F.D., Kayano, M.T., & Bonfim, O.E.T. Homogeneidade, Eventos Extremos e suas Causas Climáticas: Bacia Hidrográfica do Rio São Francisco. Revista Brasileira de Meteorologia, 2022, 37, 199-212. https://doi.org/10.1590/0102-77863710122

Sadeghi, M., Nguyen, P., Naeini, M.R., Hsu, K., Braithwaite, D., Sorooshian, S. (2021). PERSIANN-CCS-CDR, a 3-hourly 0.04° global precipitation climate data record for heavy precipitation studies. Sci Data, 8, 157. https://doi.org/10.1038/s41597-021-00940-9

Singh, T., Saha, U., Prasad, V.S., & Gupta, M.D. (2021). Assessment of newly-developed high resolution reanalyses (IMDAA, NGFS and ERA5) against rainfall observations for Indian region. Atmospheric Research, 259, 105679. https://doi.org/10.1016/j.atmosres.2021.105679.

Spinoni, J., Barbosa, P., De Jager, A., McCormick, N., Naumann, G., Vogt, J.V., Magni, D., Masante, D., & Mazzeschi, M. (2019). A new global database of meteorological drought events from 1951 to 2016. Journal of Hydrology: Regional Studies, 22, 100593. https://doi.org/10.1016/j.ejrh.2019.100593.

Taylor, K.E. (2001). Summarizing multiple aspects of model performance in a single diagram. Journal of Geophysical Research, 106, 7183–7192. https://doi.org/10.1029/2000JD900719

Tirivarombo, S., Osupile, D., & Eliasson, P. (2018). Drought monitoring and analysis: Standardized Precipitation Evapotranspiration Index (SPEI) and Standardized Precipitation Index (SPI). Physics and Chemistry of the Earth. https://doi.org/10.1016/j.pce.2018.07.001

Verhoeven, E., Wardle, G.M., Roth, G.W., & Greenville, A.C. (2022). Characterizing the spatiotemporal dynamics of drought and wet events in Australia. Science of The Total Environment, 846, 157480. https://doi.org/10.1016/j.scitotenv.2022.157480.

Yang, X., Zhou, B., Xu, Y., & Han, Z. (2021). CMIP6 evaluation and projection of temperature and precipitation over China. Advances in Atmospheric Sciences, 38, 817-830. https://doi.org/10.1007/s00376-021-0351-4

Authorship contributions

1 – Osmar Toledo Bonfim
PhD in Meteorology
https://orcid.org/0000-0001-8863-8313 • osmartoledob@gmail.com
Contribution: Conceptualization, Methodology, Software, Data Curation, Investigation, Writing – Original

2 – Vanessa Ferreira
PhD in Meteorology
https://orcid.org/0000-0001-7705-3782 • vanessaferreirameteorologia@gmail.com
Contribution: Methodology, Formal Analysis, Investigation, Writing – Original Draft, Writing – Review Editing

3 – Rafael Maroneze
PhD in Physics
https://orcid.org/0000-0002-3025-9676 • rafaelmaroneze@unipampa.edu.br
Contribution: Software, Validation, Data Curation, Supervision, Project Administration

4 – Roilan Valdes
MSc in Physics
https://orcid.org/0009-0005-6357-345X • roilan.valdes@engie.com
Contribution: Resources, Data Visualization, Project Administration, Funding Acquisition

5 – Luca Mortarini
PhD in Physics
https://orcid.org/0000-0002-0543-2975 • l.mortarini@isac.cnr.it
Contribution: Writing – Review Editing, Supervision

How to cite this article

Bonfim, O. T., Ferreira, V., Maroneze, R., Valdes, R., & Mortarini, L. (2026). Characterizing the 2019-2021 drought in Southern and Southeastern Brazil using S-TRACK method. *Ciência e Natura*, v.48, e83931. https://doi.org/10.5902/2179460X87939